Original Paper

Neuro
-endocrinology

Neuroendocrinology
DOI: 10.1159/000321119

Received: August 18, 2010
Accepted after revision: September 8, 2010
Published online: October 9, 2010

Effects of Estrogen on Beta-Amyloid-Induced Cholinergic Cell Death in the Nucleus Basalis Magnocellularis

Éva M. Szegő[a–c] Attila Csorba[b] Tamás Janáky[b] Katalin A. Kékesi[a]
István M. Ábrahám[a] Gábor M. Mórotz[a] Botond Penke[b] Miklós Palkovits[d]
Ünige Murvai[e] Miklós S.Z. Kellermayer[e] József Kardos[f] Gábor D. Juhász[a]

[a]Laboratory of Proteomics, Eötvös Loránd University, Budapest, [b]Medical Chemistry Department, University of Szeged, Szeged, Hungary; [c]Department of Neurodegeneration and Restorative Research, Georg-August University, DFG Research Center Molecular Physiology of the Brain (CMPB), Göttingen, Germany; [d]Neuromorphological and Neuroendocrine Research Laboratory, Department of Anatomy, Histology and Endocrinology, Semmelweis University and the Hungarian Academy of Sciences, [e]Department of Biophysics and Radiation Biology, Semmelweis University, and [f]Department of Biochemistry, Eötvös Loránd University, Budapest, Hungary

Key Words
Alzheimer disease · Estrogen · Amyloid · Micropunch · Proteomics · MAPK pathway · Differential two-dimensional gel electrophoresis · Nucleus basalis magnocellularis

Abstract
Alzheimer disease is characterized by accumulation of β-amyloid (Aβ) and cognitive dysfunctions linked to early loss of cholinergic neurons. As estrogen-based hormone replacement therapy has beneficial effects on cognition of demented patients, and it may prevent memory impairments, we investigated the effect of estrogen-pretreatment on Aβ-induced cholinergic neurodegeneration in the nucleus basalis magnocellularis (NBM). We tested which Aβ species induces the more pronounced cholinotoxic effect in vivo. We injected different Aβ assemblies in the NBM of mice, and measured cholinergic cell and cortical fiber loss. Spherical Aβ oligomers had the most toxic effect. Pretreatment of ovariectomized mice with estrogen before Aβ injection decreased cholinergic neuron loss and partly prevented fiber degeneration. By using proteomics, we searched for proteins involved in estrogen-mediated protection and in Aβ toxicity 24 h following injection. The change in expression of, e.g., DJ-1, NADH ubiquinone oxidoreductase, ATP synthase, phosphatidylethanolamine-binding protein 1, protein phosphatase 2A and dimethylarginine dimethylaminohydrolase 1 support our hypothesis that Aβ induces mitochondrial dysfunction, decreases MAPK signaling, and increases NOS activation in NBM. On the other hand, altered expression of, e.g., MAP kinase kinase 1 and 2, protein phosphatase 1 and 2A by Aβ might increase MAPK suppression and NOS signaling in the cortical target area. Estrogen pretreatment reversed most of the changes in the proteome in both areas. Our experiments suggest that regulation of the MAPK pathway, mitochondrial pH and NO production may all contribute to Aβ toxicity, and their regulation can be prevented partly by estrogen pretreatment.

Introduction

Alzheimer disease (AD) is the most prevalent age-related neurodegenerative disease, and the most common form of dementia [1]. Besides the accumulation of β-am-

KARGER

Fax +41 61 306 12 34
E-Mail karger@karger.ch
www.karger.com

0028–3835/10/0000–0000$26.00/0

Accessible online at:
www.karger.com/nen

Eva M. Szego
Department of Neurodegeneration and Restorative Research
Georg-August University, DFG Research Center Molecular Physiology of the Brain
Waldweg 33, DE–37073 Göttingen (Germany)
Tel. +49 551 391 3547, Fax +49 551 391 3541, E-Mail eszego@uni-goettingen.de

yloid (Aβ) peptide, neurofibrillary tangles and synaptic loss [2], another characteristic of AD is the early degeneration of the basal forebrain cholinergic system (BFC) [3, 4]. Neurons of BFC express the receptor α7 nicotinic acetylcholine receptor, which binds Aβ selectively and with high affinity, making cholinergic neurons vulnerable in AD or protecting against Aβ [5–7].

AD is known to be gender dependent and age-related loss of estrogen (17β-estradiol, E2) probably increases the risk of AD [8]. E2-based hormone replacement therapy (ERT) decreased the risk of AD and cognitive dysfunctions in some clinical studies, suggesting a protective role of E2 [9–12]. Supporting these findings, E2 was found to be neuroprotective in in vitro and in vivo experimental AD models [13–16]. It is known that E2 destabilizes Aβ fibrils in vitro [17] and decreases Aβ load in transgenic mice [18]. In addition, E2 reduces Aβ-induced Ca^{2+} overload [19] and p38 mitogen-activated protein kinase (p38MAPK) activation [20] in vitro. E2 is able to optimize brain metabolism, achieving optimal energy consumption during different mental functions [21–23]. Moreover, E2 treatment improves cognitive performance partly via interaction with the basal forebrain cholinergic system [24, 25]. However, despite the beneficial effects of E2 found in animal studies or reported from human trials, some studies demonstrated that ERT has no effect on cognitive performance and on severity of dementia in female patients [26, 27], meaning that ERT is still controversial for the treatment of dementia.

Both Aβ and E2 generate widespread changes in the brain by controlling gene expression among others [22, 28–31], inducing cell death or preparing cells for toxicity and altering cellular reactions to Aβ. In our present study, by searching for possible target proteins, we aimed to find the mechanisms and raise a hypothesis underlying Aβ toxicity on cholinergic neurons and the possible neuroprotective effects of E2 in vivo. Hence, we first determined the neurotoxic potential of differently aggregated Aβ1–42 solutions on the mouse nucleus basalis magnocellularis-substantia innominata (NBM-SI) cholinergic neurons in vivo. We measured cholinergic cell loss in the NBM-SI, and cholinergic fiber density in the projection area (somatosensory cortex, SSCTX, layer V). After selection of the most potent Aβ solution, in the second part of our experiments, we investigated the effect of E2 pretreatment on Aβ cholinotoxic effects. In addition, we performed a proteomic investigation to find the proteins influenced by Aβ and Aβ after E2 pretreatment. In this study, we present the possible mechanisms explaining Aβ toxicity and the protective effects of E2 against Aβ on NBM-SI cholinergic neurons.

Methods

Animals

Animal breeding and experiments were performed based on the rules of the Local Animal Care Committee at the Eötvös Loránd University, in accordance with the European Union conforming to the Hungarian Act of Animal Care and Experimentation. Female wild-type C57BL6/J mice were maintained under a 12-hour light/dark cycle at 20°C, and were supplied with water and food ad libitum.

In vitro Characterization of Aβ Solutions: Atomic Force Microscopy and Thioflavin T Measurements

Aβ1–42 (a gift from Márta Zarándi [32]) peptide was dissolved in 100% hexafluoro-isopropanol (HFIP) for 6 h to prepare a monomer solution [33]. The monomer solution was centrifuged at 15,000 *g* (10 min), and the supernatant was lyophilized and kept at –80°C until use. The morphology and size of the Aβ aggregates in vitro was determined using atomic force microscopy (AFM). Aβ samples at 600 μM concentration in glucose-free artificial cerebrospinal fluid (ACSF, in mM: 144 NaCl; 3 KCl; 1 $MgCl_2$; 2 $CaCl_2$; pH 7.3) were incubated for 0, 12, 24 and 48 h at room temperature. As the samples with 24 and 48 h incubation time did not adhere sufficiently to the mica surface (Electron Microscopy Sciences, Hatfield, Pa., USA), they were diluted in deionized water (15- to 30-fold) and the solutions were then incubated on the mica surface for 2 min and replaced with water. These solutions were measured in water instead of ACSF. Images were obtained under similar conditions with an MFP3D AFM instrument (Asylum Research, Santa Barbara, Calif., USA), operating in a noncontact mode, using the Olympus BioLever silicon nitride cantilever (Olympus Co., Japan); typical resonance frequency: ~9 kHz. Drive amplitude and contact force were kept to a minimum. Areas were scanned at 0.5–1 Hz rate. Images were evaluated by measuring the height of 100–200 individual aggregates above the mica surface using MFP-3D software (Asylum Research). Objects clearly associated from a large number of aggregates were taken as sample preparation artefacts and were excluded from the measurements. It is important to note that AFM measurements may underestimate the diameter of Aβ structures because of sample compression by the AFM probe [34]. However, the technique is excellent to follow the progress of aggregation and the change in morphology.

For thioflavin T (ThT) fluorescence measurements, 1-μl aliquots were taken from the samples and mixed with 1.0 ml of 5 μM ThT (Sigma) in 50 mM glycine-NaOH buffer at pH 8.5 [35]. ThT fluorescence was monitored immediately at 485 nm with excitation at 445 nm in a cell thermostatted to 25°C using a SPEX FluoroMax instrument (Jobin-Yvon, Longjumeau Cedex, France). Excitation and emission bandwidths were set to 5 nm. Data are from 5 measurements/time point.

Preparation of Tissue Sections for Toxicity Measurements of Aβ Assemblies

To prepare different Aβ aggregates suitable for in vivo experiments, the lyophilized samples were dissolved in ACSF at a concentration of 600 μM and kept at room temperature for 0, 12, 24 or 48 h prior to administration. The concentration of the Aβ solution was determined in a preliminary experiment, and we selected the lowest concentration to achieve a minimum of 25% cholin-

ergic cell death (data not shown). In order to eliminate the possible interference of endogenous estrogen with Aβ toxicity, adult female 45- to 60-day-old mice were bilaterally ovariectomized (OVX) under deep anesthesia using Avertin (2% 2,2,2-tribromoethanol, 1,2% amyl-hydrate; 8% ethanol in physiological saline; Sigma, USA). In the first set of experiments, we aimed to determine the cholinotoxic effect of different Aβ assemblies. Aβ was incubated in ACSF for 0, 12, 24 or 48 h at room temperature prior to injecting. On post-OVX day 14, 2 × 1 μl 600 μM Aβ solution or ACSF was injected slowly into the NBM-SI using fused silica capillary (coordinates: L –2/+2, AP –0,65, DV –4,1/–4,3) [36]. During stereotactic surgery, mice were in deep anesthesia (1.5% halothane in air, 1.8 liters/min flow rate). ACSF was injected randomly into one side, and Aβ solution into the other side of the brain; therefore, the same animal served as its own control (ACSF-injected site, n = 5/group). On post-OVX day 29, mice were anesthetized by a lethal dose of Avertin, and transcardially perfused with 4% paraformaldehyde (Merck, Germany), pH 7.6 in phosphate-buffered saline solution. Brains were removed, post-fixed for 2 h at 4°C and cryoprotected in Tris-phosphate-buffered solution (TBS), pH 7.6, containing 30% sucrose overnight at 4°C. 30-μm coronal sections were cut on a freezing microtome and four sets of sections were collected in TBS.

Determination of the Effect of E2 on Aβ Toxicity in vivo

To study the effects of E2 pretreatment on the Aβ-exerted cholinotoxicity, the following procedures were used. 45- to 60-day-old mice were bilaterally ovariectomized (see above section). On post-OVX day 14, animals received a subcutaneous injection of 1 μg of 17β-estradiol (E2; in 0.1 ml ethyl-oleate vehicle, Sigma) or the same volume of vehicle (EO). Twenty-four hours after the EO/E2 treatment, the previously prepared Aβ solution (2 × 1 μl, 600 μM in ACSF, 24-hour incubation at room temperature) or ACSF was injected slowly into the NBM-SI (see the previous section). Altogether, 12 mice were treated with EO and Aβ and 12 mice with E2 and Aβ. Six EO-Aβ-injected and 6 E2-Aβ-injected mice were used for differential two-dimensional gel electrophoresis (DIGE) experiments (n = 6). These mice were sacrificed 24 h after the Aβ-injection (post-OVX day 16) by cervical dislocation, brains were rapidly removed (<40 s) and frozen in dry ice. Serial 100-μm coronal cryosections were cut at –10°C and tissue samples corresponding to the SSCTX and the NBM-SI were dissected using the 'punch technique' [37] according to a microdissection map [38]. Samples were stored at –80°C until use. Six EO-Aβ-, and six E2-Aβ-injected mice were used for the regeneration study (n = 6). These mice were sacrificed on post-OVX day 30, perfused, and their brains treated as described above.

Protein Isolation, Differential Two-Dimensional Gel Electrophoresis and In-Gel Digestion

Eight different sets of tissue samples were collected for proteomic studies: four from EO-treated mice (SSCTX and NBM-SI from the ACSF-injected side and SSCTX and NBM-SI from the Aβ-injected site), pieces of tissue from 6 different animals, therefore 6 pieces/area/treatment group, and the same areas from the E2-treated animals (6 mice). Tissue samples were homogenized as we reported earlier [23]. The pH of the supernatant corresponding to cytosolic and membrane fractions was adjusted to 8.0. Five microgram of each protein sample was labeled with Cy5 saturation dye CyDye DIGE Fluor-Labeling Kit for Scarce Samples (4 nmol/5 μg protein, GE Healthcare, Uppsala, Sweden) according to the manufacturer's instructions. The reference sample (internal standard, equal amounts: 5 μg of protein from all E2- and all EO-treated samples from the same region) was labeled with Cy3 and the two differently marked samples (5 μg of Cy5-labeled sample and 5 μg Cy3-labeled reference) were multiplexed to be resolved in the same gel. Labelled proteins were separated and visualized as described previously (DryStrip pH: 4–7, 10% acrylamide gel) [23]. Differential protein analysis was performed using DeCyder software package 6.0, DIA and BVA modules (GE Healthcare). For the identification of proteins in spots of interest, preparative 2D electrophoresis was performed separately using 800 μg of proteins per gel [23].

LC-MS Analysis and Protein Identification and Extended Literature Search

LC-MS analysis was performed by an Agilent HPLC-Chip/MS system consisting of 1100 Series HPLC system and a 6330 LC/MSD XCT Plus ion trap mass spectrometer. The LC system was operated in a sample enrichment/desalting mode using a ProtID-Chip-43 (II Chip-Column) (column material: ZORBAX 300 SB-C18 5 μm, trap column volume: 40 nl, analytical column: 43 × ID 0.075 mm). The HPLC solvents were the following: solvent A: 0.1% formic acid in water and solvent B: 0.1% formic acid in acetonitrile. Two microliter of sample was enriched with solvent A at a flow rate of 4 μl/min for 2 min using a capillary pump then followed by gradient elution of tryptic peptides at a flow rate of 300 nl/min using a nano pump. The gradient was 5% B/min increase of concentration B from 5 to 45% under 10 min followed by a gradient column-wash from 60 to 90% solvent B in 2 min. The mass spectrometer was operated in the autoMSMS mode, the resolution was less than 0.5 u (FWHM) and the scan speed was 8,100 u/s. The survey scan range was 300–1,600 m/z and 4 ions were selected for CID. MSMS scan range was set to 100–1800 m/z at 26,000 u/s at a resolution of less than 0.6 u (FWHM). All acquired MSMS data were processed and subjected to database search by Agilent Spectrum Mill MS Proteomics Workbench Ver. A.03.02 against NCBInr (11/16/2009 database). Database search parameters were set to 1.5 Da for precursor ion mass tolerance, 0.6 Da for fragment ion mass tolerance. Constant modification of Cys was specified as carbamidomethylation, variable modifications were set to methionine oxidation, deaminated glutamine, acetylation of protein N-terminal and oxidation of tryptophan. For protein assignment the minimum score was set to 20 for proteins and peptide hits were accepted above score of 9, 10, 11 and 12 according to their charge state of 1+, 2+, 3+ and 4+, respectively [39]. To make a functional interpretation of our data, a systematic literature survey was conducted [23].

Immunohistochemistry and Acetylcholinesterase Histochemistry

To detect cholinergic neurons, free-floating, peroxidase-based immunohistochemistry was performed in the same manner we reported previously with only a slight modification [40]. We used anticholine acetyl-transferase (anti-ChAT antibody (1:2000), Santa Cruz Biotechnology, Calif., USA) for 48 h at 4°C. For fluorescent labeling of calbindin (1:3,000, Swant, Switzerland) and ChAT (1:1,000), we used florescent dye-conjugated secondary antibodies (1:1,000, AlexaFluor-488 for ChAT and AlexaFluor-555 for calbindin; Invitrogen, Calif., USA). Visualization of acetyl-

cholinesterase fibers was done according to the method of Hedreen et al. [41].

Data Analysis and Statistics

Number of ChAT-ir cells were counted by an Olympus BX51 microscope (Olympus Optical, Hamburg, Germany) using ×40 objectives. Every fourth section was stained and ChAT-ir neurons of the NBM-SI were counted from both sides (ACSF- or Aβ-injected sides from four sections) by an investigator blind to the experimental groupings; finally, the number of neurons/μm^3 and the percentage change was determined. Data are expressed as mean ± SEM. ANOVA was carried out to examine the effects of EO/E2 and ACSF/Aβ treatment (R software packages, version 2.8.0, R Development Core Team 2008, Vienna, Austria).

Acetylcholinesterase (AChE) fiber density was determined in the SSCTX, layer V. As the cholinergic neurons of the NBM project almost exclusively unilaterally to the SSCTX, it allowed us to determine the differences between ACSF- and Aβ-injected sides in the same animal. Every fourth section was stained and six sections were analyzed per animal. Six images were taken of every slice using a ×100 objective (Olympus BX51) and the area covered by AChE fibers was measured ten times from the same image following background subtraction and binarization. Therefore, six sections/animal, six images/section and 10 measurements/image resulted in a hierarchical nested design. The effect of Aβ on fiber density was expressed as a percentage change relative to the ACSF-injected side. A generalized linear mixed model was applied, the dependent variable was the fiber density, and the independent variables were the EO or E2 treatment and ACSF or Aβ injection. The identification of animals, sections and images were set as random factors (R software).

For the DIGE experiments, ANOVAs were calculated by the DeCyder software Biological Variance Analysis (BVA module). The internal standard was a pool of equal amounts of all samples (from all SSCTX or all NBM-SI within the experiment); it was representative of every protein present and was the same across all gels from the same region. The standard provided an average image against which all other gel images were normalized, removing much of the experimental variation and reducing gel-to-gel variation.

Results

In vitro Characterization of Aβ(1–42) Aggregate Size and Morphology

Samples with 0 h incubation time mainly contained particles exhibiting a height not exceeding 1 nm (approximately 73%; fig. 1a, b). This size range possibly corresponds to the monomer state of Aβ, while particles larger than 1 nm could be assigned to the aggregated forms of Aβ peptide [33]. The percentage of the small particles significantly decreased with incubation time to approximately 50, 25 and 5% after 12, 24 and 48 h, respectively (fig. 1a, b). We observed a greater portion of large particles after longer incubation times. After 12 h incubation, the ratio of particles with 1–2 nm height increased, a form corresponding to small oligomers [33]. Aggregates formed in the 2–4 nm range appeared after longer incubation times (24 and 48 h) with a maximum occurrence at 2.3–2.5 nm (fig. 1a, b). We observed a change in the morphology of the aggregates paralleling their increased size. Spherical aggregates appeared in the 24-hour samples (fig. 1b), while after 48 h, besides spherical oligomers, short, fibrillar structures were formed with 50–200 nm length and average height of 2.5–3 nm (fig. 1b). The latter species of aggregates could not have been mature amyloid fibrils because of their shortness and small diameter. Rather, these were protofibrils formed from oligomers.

Thioflavin T is a fluorescent dye that binds to protein aggregates, especially to amyloid fibrils, while it does not bind to monomers. Upon binding, it shows high fluorescence intensity. 0-hour samples exhibited low ThT fluorescence intensity reflecting the high monomer content in the solution (fig. 1c). 12-, 24- and 48-hour samples exhibited an increasing ThT fluorescence intensity with time indicating the progress of the aggregation process and an increase in the amyloid-like structure content (fig. 1c).

Determination of the Cholinotoxic Potential of Different Aβ Forms

Injection of the 0-hour solution had no effect on the number of cholinergic cells in the NBM-SI (fig. 2a) and failed to induce cholinergic fiber loss in the SSCTX (fig. 2b). In contrast, the cholinotoxic potential of the different Aβ solutions increased with pre-incubation time (loss of neurons = counted control site-counted lesioned site; 12-hour solution: approximately 15% cell loss, $p = 0.033$; 24-hour solution: approximately 25% cell loss, $p = 0.002$; 48-hour solution: approximately 26% cell loss, $p = 0.002$) although the 48-hour sample had the same effect as the 24-hour sample ($p = 0.679$; fig. 2a). Similarly, fiber

Fig. 1. In vitro characterization of size distribution and morphology of Aβ 1–42 aggregates. **a** Representative AFM images of Aβ samples after incubation for 0, 12, 24 and 48 h, respectively. Scale bars represent 200 nm. Color codes for height traces are presented. **b** Height distributions of Aβ samples (AFM measurements) after different incubation times at room temperature. Columns represent the percentage of individual aggregates of a certain height 0.2 nm interval. Large objects >6 nm were excluded from calculation. **c** Changes in the intensity of thioflavin T fluorescence show increasing aggregation of Aβ1–42 with time. ThT binds protein aggregates, but not monomers. Data are from 5 measurements/time point.

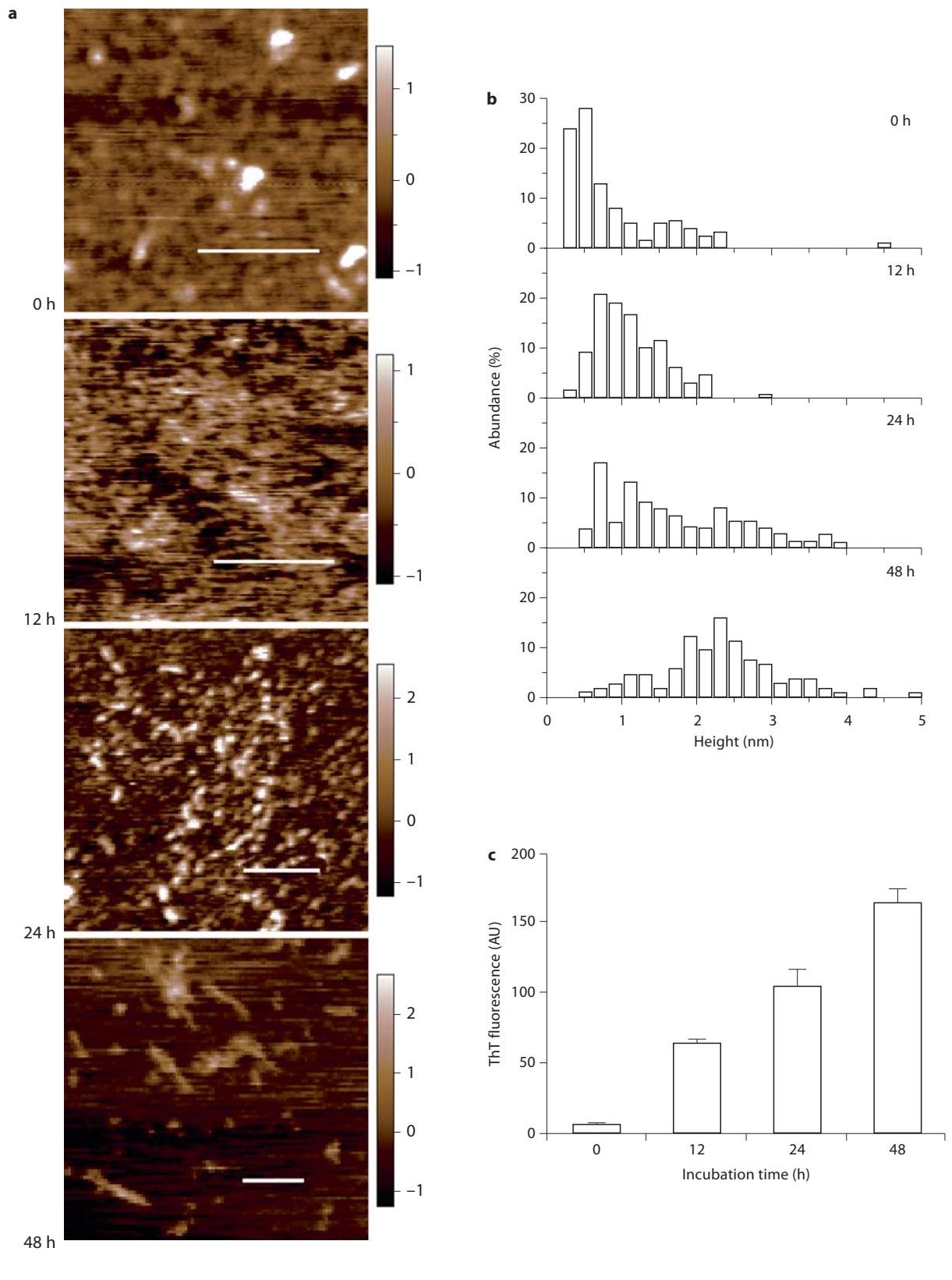
a
0 h
12 h
24 h
48 h
1
0
−1
2
1
0
−1
b
0 h
12 h
24 h
48 h
Abundance (%)
Height (nm)
c
ThT fluorescence (AU)
Incubation time (h)

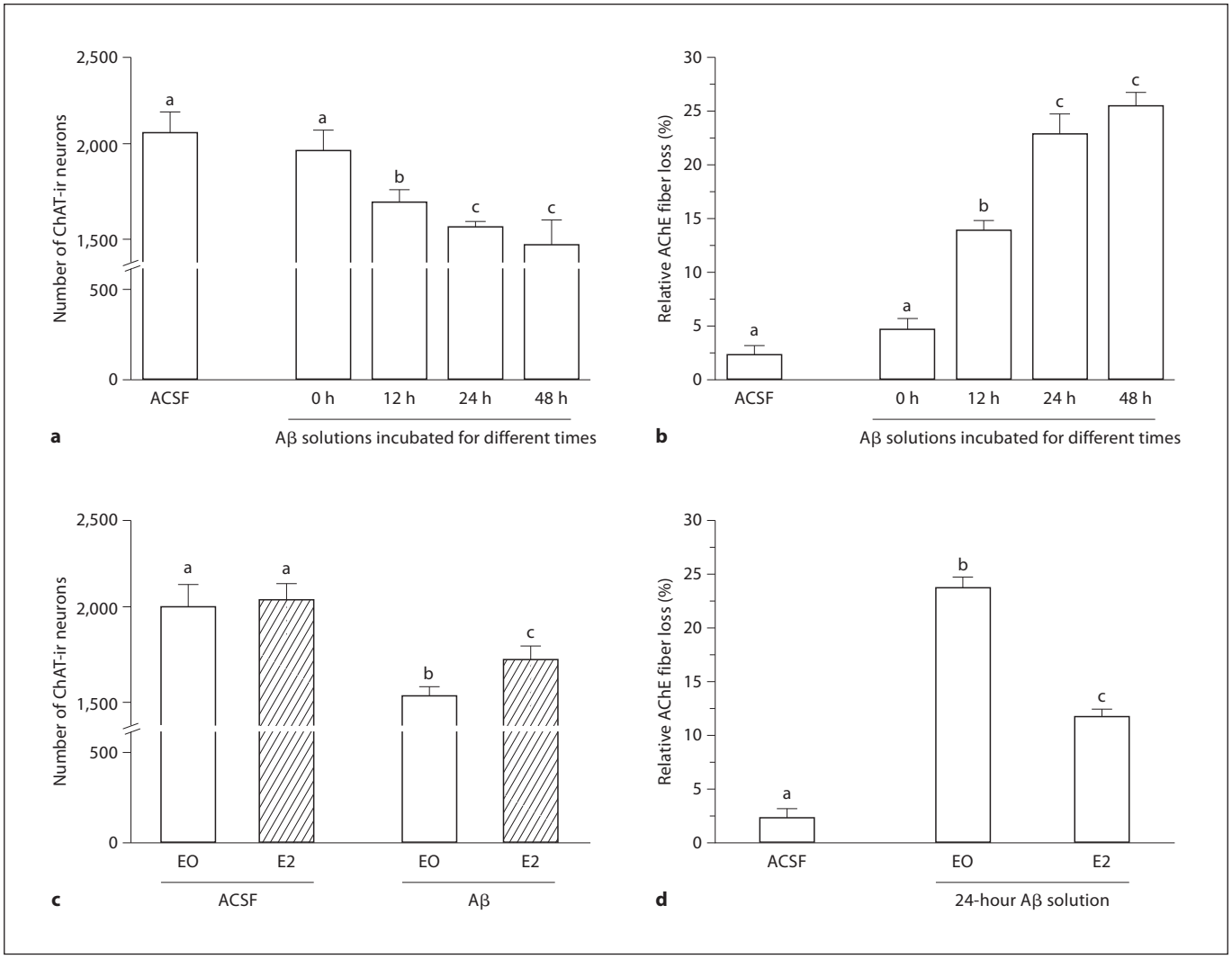

Fig. 2. Effects of incubation time of Aβ solution and E2 pretreatment on unilateral NBM lesions induced by Aβ. **a**, **b** The toxic effect of the 600 μM Aβ solution increases with preincubation time. Quantitative analysis of cholinergic cell number ChAT-ir (**a**) and area fraction covered by cholinergic AChE-positive fibers (**b**) revealed an increasing toxic effect of Aβ solution with increasing incubation time. AChE fiber density was measured in the layer V of the SSCTX, and fiber loss is presented as a relative percentage of the ACSF-injected contralateral side. Maximum neuron and fiber loss was found after 24 or 48 h incubation time of Aβ. **c** 24 h E2 pretreatment did not increase cholinergic cell numbers, as we found comparing the contralateral ACSF-injected sides of EO-treated mice (open bars) and E2-treated mice (diagonal bars). E2 decreased the vulnerability of cholinergic cells to Aβ lesion compared to EO pretreatment ipsilateral sides. **d** E2 pretreatment significantly decreased Aβ-induced AChE fiber loss in the SSCTX. Different letters show significant differences, $p < 0.05$. Data are expressed as mean ± SEM, n = 5 (**a**, **b**) or n = 6 (**c**, **d**).

loss increased in the SSCTX parallel with the increasing incubation time of the Aβ solutions (fiber loss = measured control SSCTX-measured lesioned SSCTX; 12-hour solution: approximately 14% fiber loss, p = 0.014; 24-hour solution: approximately 23% fiber loss, p = 0.002; 48-hour solution: approximately 26% fiber loss, p = 0.0002; fig. 2b) and the 24- and 48-hour Aβ solutions induced equal cholinergic fiber loss (p = 0.153). Comparing the size, morphology (fig. 1) and in vivo effect of the different Aβ solutions the observed toxicity (fig. 2a, b) could not be related to monomers in our model. Moreover, the similar toxic effect of 24- and 48-hour samples suggests that the most effective components are not mature aggregates, since thioflavin T binding (hence aggregation) in-

creased with time (fig. 1c). Our data also indicate that toxic species are not protofibrils since these particles are missing from the 12- and 24-hour samples (fig. 1a, b). Based on our in vivo and in vitro experiments, we suggest that the most toxic species are not the protofibrils, but rather the spherical oligomer forms in the size range of 1–3 nm.

Pretreatment with 17β-Estradiol Has a Protective Effect against Aβ

We selected the 24-hour incubation time for the further experiments, as this Aβ solution (and the 48-hour solution) had the more pronounced cholinotoxic effect. Pre-treatment with EO vehicle had no effect on the Aβ toxicity (cell loss after Aβ: approximately 23%, $p = 0.001$; fiber loss: approximately 25%, $p = 0.0009$, compared to the ACSF-injected site; fig. 2c, d). E2 significantly decreased the cytotoxic effect of Aβ compared to EO treatment (approximately 15 vs. 23% cell loss, $p = 0.026$), although it did not eliminate the toxic effect ($p = 0.003$, comparison of E2- and ACSF-treated sides). Parallel with decreased neuron loss, E2 pretreatment reduced Aβ-induced cholinergic fiber loss in the SSCTX (approximately 12 vs. 25% fiber loss, $p = 0.00006$, fig. 2d), but it could not eliminate the Aβ toxicity ($p = 0.002$, comparison of E2-ACSF and E2-Aβ). The similar change in the Aβ-induced cell and fiber loss after E2 pretreatment suggests that E2 had no regenerative effect, rather a neuroprotective capacity.

Identification of Differentially Expressed Proteins after Aβ or E2-Aβ Treatment

In this experiment, we aimed to find proteins and possible early pathways influenced by Aβ or Aβ+E2 treatment, right after Aβ injection. Usually, changes in the expression of structural proteins occur in successive steps, but as a delayed response. Therefore, we analyzed protein expression pattern 24 h after Aβ injection using differential two-dimensional gel electrophoresis (DIGE) and mass spectrometry.

Altogether 1,440 spots were present on the master gel from samples of the SSCTX, and 1,723 from the NBM-SI as we determined using DeCyder software. Forty-eight hours after E2 and 24 h after Aβ treatment, the majority of protein spots showed only small changes between groups. However, a two-way ANOVA across all the gels showed a significant difference in the intensity of 127 spots in the NBM-SI and 95 in the SSCTX. We could identify 56 proteins from the 127 spots of the NBM-SI samples and 35 proteins from 95 spots of the SSCTX. Representative 2-D gel maps and 3D reconstruction of protein spots are shown in figure 3. Identified proteins, showing significant differences, are listed in tables 1 and 2. We used the EO vs. E2 and ACSF vs. Aβ samples as independent variables in the analysis and could thereby make four reasonable comparisons between groups: (1) EO-ACSF vs. EO-Aβ, (2) E2-ACSF vs. E2-Aβ, (3) ACSF vs. Aβ, and (4) EO-Aβ vs. E2-Aβ. Hereafter, we concentrate on the comparison of animals treated with (1) EO-Aβ vs. EO-ACSF, as this comparison gives us information about the mechanism of Aβ toxicity (injected into the NBM-SI) and (4) EO-Aβ vs. E2-Aβ, as this later analysis may provide evidence about the protective effects of E2 against Aβ. Regarding just these comparisons, we could identify 42 protein changes in the NBM-SI (table 1), and 27 changes in the SSCTX (table 2). We clustered the identified proteins into seven functional groups, namely 'antioxidant defence', 'cytoskeleton', 'metabolism', 'protein turnover and stability', 'signaling', 'synaptic processes' and 'unknown'.

We could identify proteins from the NBM involved in the regulation of the redox homoeostasis (table 1): expression of protein disulfide isomerase associated 3 and dimethylarginine dimethylaminohydrolase 2 decreased, while level of DJ-1 protein increased after Aβ injection, suggesting a decreased antioxidant level. In contrast, 24-hour E2 pretreatment reversed these changes, and increased the expression of two further proteins (inner membrane protein and glutathione S-transferase). Aβ induced changes in the expression of cytoskeletal proteins (dihydropyrimidinase-like 2, fascin and γ-actin), while E2 prevented or reversed these changes. Changes in the proteins involved in general cellular metabolism were also observed, and Aβ-induced changes were prevented or reversed by E2 pretreatment. Interestingly, Aβ decreased expression of otubain-1 and protesome 26S subunit, proteins involved in protein degradation, while E2 pretreatment prevented these changes. Proteins involved in intracellular signaling (e.g. protein phosphatase 2A) or Ca^{2+} buffering (calbindin) were also identified as targets of Aβ or E2.

Proteins involved in antioxidant defense were identified from SSCTX samples (table 2) after Aβ injection. Expression of dimethylarginine dimethylaminohydrolase 1 and sepiapterin reductase increased, while protein disulfide isomerase associated 3 decreased after Aβ injection. E2 pretreatement reversed these changes. Expression of some cytoskeletal proteins like dihydropyrimidinase-like 2 and septin 8 decreased, while γ-actin increased after Aβ-injection. E2 pretreatment before Aβ injection

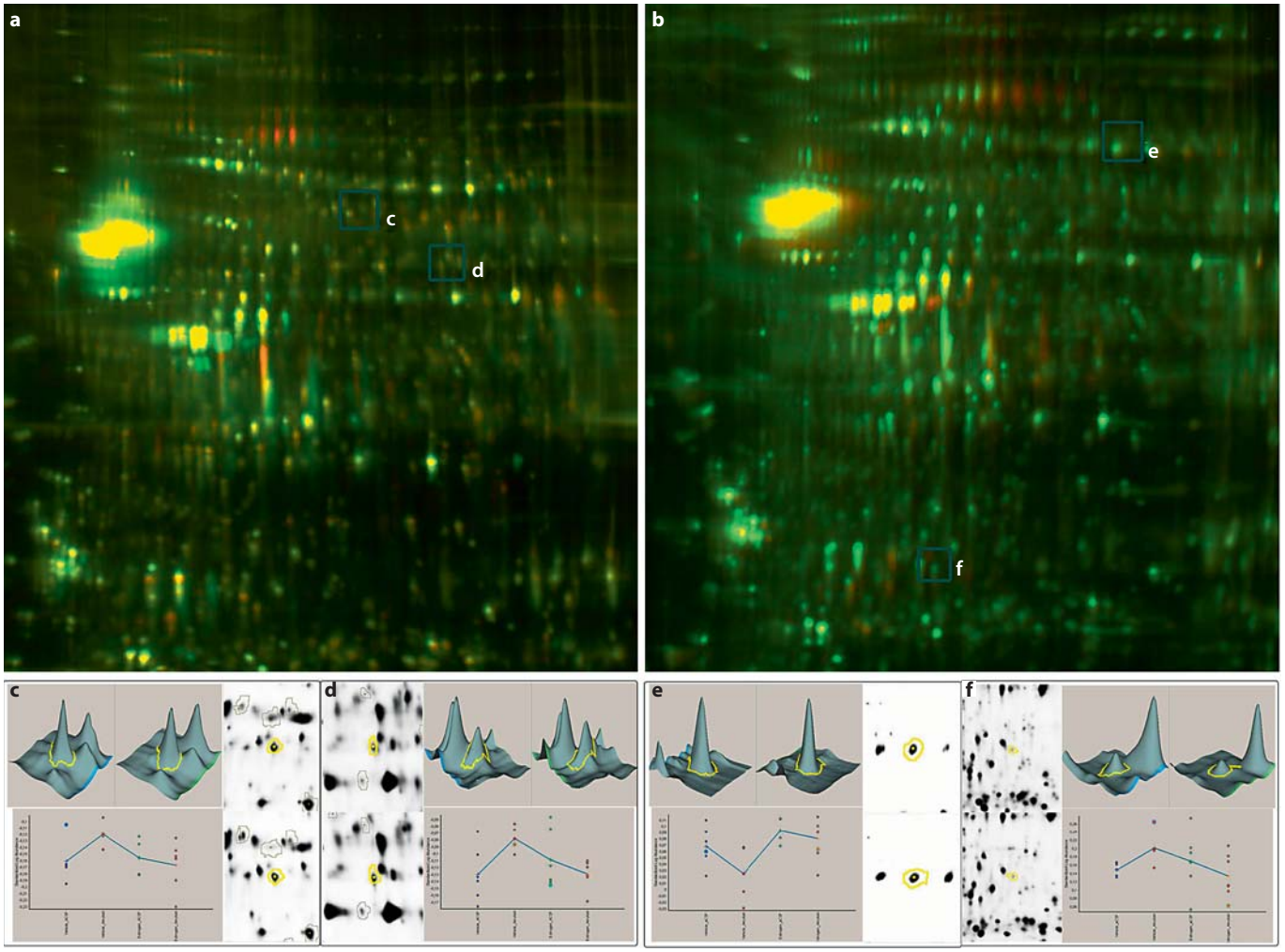

Fig. 3. Representative 2D gel images from the NBM-SI (**a**, **c**, **d**) and SSCTX (**b**, **e**, **f**). **a**, **b** Pseudo-colored 2D maps of NMB-SI and SSCTX, respectively. The internal standard pooled from all of the samples from the same anatomical area was labeled with Cy3 green, samples from the treatment group Aβ-EO were labeled with Cy5 red. **c–f** 3D reconstruction of protein spots marked in (**a**) or (**b**) gel maps. Graphs represent the abundance of the spot relative to the internal standard.

prevented these changes, and increased the expression of septin 3 protein. A relatively low number of proteins was identified from the 'metabolism' groups, meaning that Aβ had a lower effect on general cellular homeostasis outside of the injection site. Interestingly, we found Aβ-induced upregulation of apolipoprotein A-1, while E2 pretreatment decreased the expression of this protein. Proteins with chaperon activity (e.g. heat shock protein 105 kDa, stress protein 70) were also altered by Aβ or E2 × Aβ treatment, moreover, expression of macropain subunit 28 increased after Aβ injection, but decreased with E2–Aβ treatment. In contrast to the findings from the NBM, we observed increased MEKK1 and decreased protein phosphatase 2A expression, suggesting the activation of ERK pathways following Aβ injection. Secernin 1, a protein involved in synaptic processes, decreased, while EH domain containing 3 increased in expression following Aβ injection, and E2 treatment reversed these changes.

Decreased Calbindin Immunoreaction in the NBM-SI after Aβ Injection

We selected calbindin from the protein list to check the expression pattern after Aβ injection of EO- and E2-treated mice. We found no colocalization of calbindin

Table 1. Proteins identified from NBM-SI after Aβ or E2-Aβ treatment

Spot No.	Protein	Accession No.	EO-ACSF vs. EO-Aβ		EO-Aβ vs. E2-Aβ		MW	PI	% Seq.
			p value	Av. ratio	p value	Av. ratio			
Antioxidant defense									
SI0210	inner membrane protein, mitochondrial	70608131	0.3	–1.12	**0.044**	**1.19**	86295.4	7.02	5
SI0482	protein disulfide isomerase associated 3	112293264	**0.042**	**1.1**	**0.03**	**–1.11**	56678.7	5.88	5
SI1474	N(G),N(G)-dimethylarginine dimethylaminohydrolase 2	45476968	**0.048**	**1.07**	**0.037**	**–1.07**	29646	5.66	6
SI1633	DJ-1 protein	74212240	**0.0013**	**–1.07**	**0.039**	**1.12**	20025.4	6.32	12
SI1669	glutathione S-transferase, alpha 4	160298217	0.37	–1.14	**0.016**	**1.31**	26890.5	6.02	13
Cytoskeleton									
SI0254	dihydropyrimidinase-like 2	40254595	**0.03**	**1.44**	0.12	–1.27	62277.9	5.95	13
SI0256	dihydropyrimidinase-like 2	40254595	**0.038**	**1.4**	0.23	–1.24	62277.9	5.95	29
SI0381	dihydropyrimidinase-like 2	40254595	**0.049**	**–1.12**	0.44	–1.05	62277.9	5.95	5
SI0633	fascin	497775	**0.021**	**1.28**	**0.041**	**–1.33**	54508.3	6.44	5
SI0886	gamma-actin	74191566	**0.036**	**–1.18**	**0.028**	**1.17**	41811.1	5.29	15
Metabolism									
SI0212	NADH-ubiquinone oxidoreductase 75-kDa subunit, mitochondrial	47117271	**0.017**	**1.29**	0.67	–1.04	79777.3	5.51	4
SI0433	creatine kinase, brain	74223625	**0.016**	**–1.88**	0.54	–1.07	42753.5	5.46	4
SI0625	aldhehyde dehydrogenase family 5, subfamily A1	27369748	**0.0082**	**1.17**	0.37	–1.14	55968.5	8.53	4
SI0660	aldehyde dehydrogenase family 7, member A1	188219757	0.82	–1.06	**0.044**	**1.13**	58861.8	7.16	10
SI0665	enolase 2, gamma neuronal	70794816	**0.025**	**1.12**	**0.002**	**–1.13**	47141.1	6.37	7
SI0685	ATP synthase, H+ transporting, mitochondrial F1 complex, alpha subunit, isoform 1	74211977	**0.037**	**–1.42**	0.85	1.03	59782.9	9.22	5
SI0817	succinate-coenzyme A ligase, ADP-forming, beta subunit	74151797	**0.05**	**1.18**	0.45	–1.05	50797	7.7	11
SI1191	lactate dehydrogenase B	6678674	**0.0092**	**1.1**	0.11	–1.04	36572.5	5.7	5
SI1194	lactate dehydrogenase B	6678674	**0.048**	**1.12**	0.13	–1.06	36572.5	5.7	23
SI1310	malate dehydrogenase 1, NAD (soluble)	254540027	0.19	1.07	**0.036**	**–1.07**	40059.5	7.07	7
SI1414	tyrosine 3-monooxygenase/tryptophan 5-monooxygenase activation protein, ε polypeptide	26344914	**0.0016**	**–1.34**	0.4	1.07	28212	4.81	30
SI1503	phosphoglycerate mutase 1	114326546	0.12	1.07	**0.029**	**–1.11**	28832.1	6.68	32
SI1643	haloacid dehalogenase-like hydrolase domain containing 2	74190684	0.79	1.01	**0.046**	**–1.2**	28760.4	5.69	12
SI1677	ATP synthase, H+ transporting, mitochondrial F1 complex, alpha subunit, isoform 1	74211977	0.87	–1.02	**0.029**	**1.41**	59782.9	9.22	5
Protein turnover and stability									
SI0169	heat shock protein 1, alpha	74147335	**0.037**	**–1.08**	0.28	–1.04	84816.3	4.93	10
SI0720	proteasome (prosome, macropain) 26S subunit, ATPase 2	33859604	**0.0011**	**–1.45**	**0.03**	**1.38**	52866.9	5.97	8
SI0515	heat shock protein 1 (chaperonin)	148680184	**0.042**	**1.13**	0.47	–1.04	53095.7	5.3	12
SI1350	otubain 1	19527388	**0.043**	**–1.19**	0.85	1.02	31270.2	4.85	16
Signaling									
SI0676	guanosine diphosphate (GDP) dissociation inhibitor 1	74150721	0.18	1.1	**0.0062**	**–1.13**	57736.9	8.17	7
SI1313	protein phosphatase 2A, regulatory subunit B (PR 53), isoform CRA_b	26327445	**0.024**	**1.1**	**0.0067**	**–1.11**	38513.4	6.14	7
SI1467	inositol (myo)-1(or 4)-monophosphatase 1, isoform CRA_b	148673218	**0.0066**	**1.13**	0.27	1.06	31025.9	4.79	4
SI1538	calbindin 2	34098931	**0.036**	**–1.3**	0.34	1.09	31372.8	4.94	11
SI1548	calbindin 2	34098931	**0.0057**	**–1.17**	0.96	1.01	31372.8	4.94	18
SI1553	calbindin-28K, isoform CRA_a	6753242	**0.013**	**1.34**	0.54	–1.06	30093.4	4.71	24
SI0564	protein phosphatase 3, catalytic subunit, alpha isoform, isoform CRA_d	148680184	**0.038**	**–1.36**	0.11	1.22	62277.9	5.95	6
Synaptic processes									
SI0122	Aldh1l1 protein	27532959	**0.035**	**1.14**	0.37	–1.07	98734.7	5.69	2
SI0500	phosphatidylethanolamine binding protein 1	74222953	**0.049**	**1.18**	0.28	–1.11	20889.6	5.36	14
SI0572	glutamate dehydrogenase 1 precursor	6680027	0.58	–1.07	**0.0028**	**1.18**	61337.1	8.05	10
SI1307	phosphatidylethanolamine binding protein 1	74222953	**0.031**	**1.16**	0.13	–1.08	20889.6	5.36	25
SI1711	phosphatidylethanolamine binding protein 1	74222953	0.71	1	**0.0049**	**1.03**	20889.6	5.36	51
Unknown									
SI1571	mCG9061, isoform CRA_c	148706375	**0.049**	**1.14**	0.31	–1.07	28401.8	8.17	21
SI1716	RIKEN cDNA 1110067D22, isoform CRA_a	148675893	**0.027**	**1.14**	0.3	1.05	19556.5	5.48	6

Names of proteins with altered expression level after Aβ treatment are shown in blue, proteins changed after E2-Aβ treatment are in black and proteins with altered expression level after both Aβ and E2-Aβ treatments are in red. Av. ratio: ratios of protein expression levels were calculated using DeCyder software package, Biological Variance Analysis module, as the fold change between normalized spot volume of EO-ACSF- and EO-Aβ-treated samples or between EO-Aβ- and E2-Aβ-treated samples. Values below zero: decreased protein level after the specific treatment. Av. = Average; MW = molecular weight; PI = isoelectric point; MW and PI as determined by Uniprot database; % Seq.: protein sequence coverage.

Table 2. Proteins identified from SSCTX after Aβ or E2-Aβ treatment

Spot No.	Protein	Accession No.	EO-ACSF vs. EO-Aβ		EO-Aβ vs. E2-Aβ		MW	PI	% Seq.
			p value	Av. ratio	p value	Av. ratio			
Antioxidant defense									
SCTX0956	dimethylarginine dimethylaminohydrolase 1	38371755	**0.026**	**1.28**	0.11	–1.15	31381.2	5.64	5
SCTX1061	sepiapterin reductase	14714532	**0.025**	**1.13**	**0.036**	**–1.16**	27928.3	5.94	4
SCTX0387	protein disulfide isomerase associated 3	112293264	0.31	–1.17	**0.043**	**1.36**	56678.7	5.88	22
Cytoskeleton									
SCTX0137	dihydropyrimidinase-like 2	40254595	0.26	–1.16	**0.036**	**1.31**	62277.9	5.95	12
SCTX0181	dihydropyrimidinase-like 2	40254595	**0.029**	**–1.25**	0.22	1.33	62277.9	5.95	26
SCTX0196	dihydropyrimidinase-like 2	40254595	0.92	–1.02	**0.044**	**–1.16**	62277.9	5.95	19
SCTX0413	septin 8, isoform CRA_c	148701638	**0.044**	**–1.12**	0.42	1.34	57239.4	6.87	4
SCTX0706	gamma-actin	74191566	**0.049**	**1.12**	**0.015**	**–1.33**	41811.1	5.29	18
SCTX0868	neuronal-specific septin 3	4106549	0.87	1.06	**0.019**	**–1.27**	52791.9	7.45	4
Metabolism									
SCTX0096	malate dehydrogenase 1, NAD (soluble), isoform CRA_c	254540027	0.96	1	**0.039**	**1.27**	40059.5	7.07	10
SCTX0871	isocitrate dehydrogenase 3 (NAD+) alpha, isoform CRA_c	148693873	**0.047**	**–1.2**	0.73	1.04	40550	6.12	3
SCTX0986	apolipoprotein A-I	74203337	**0.044**	**1.15**	**0.014**	**–1.42**	30684.8	5.65	4
Protein turnover and stability									
SCTX0016	ubiquitin-activating enzyme E1 isoform 1	6678483	0.24	–1.17	**0.048**	**1.12**	117810	5.43	6
SCTX0021	heat shock protein 105kD	74144783	**0.039**	**–1.21**	**0.024**	**–1.59**	99209	5.46	11
SCTX0117	stress-70 protein, mitochondrial	14917005	**0.027**	**1.1**	**0.004**	**–1.68**	73528.7	5.91	25
SCTX0120	stress-70 protein, mitochondrial	14917005	0.7	1.08	**0.027**	**–1.6**	69085.2	5.44	30
SCTX0369	heat shock protein 1 (chaperonin)	183396771	0.073	–1.5	**0.048**	**–1.2**	56775.3	5.89	23
SCTX0461	stress-70 protein, mitochondrial	14917005	0.79	1.01	**0.036**	**–1.15**	73528.7	5.91	8
SCTX0581	proteasome (prosome, macropain) 28 subunit, alpha	6755212	**0.042**	**1.25**	**0.049**	**–1.04**	28673.1	5.73	5
Signaling									
SCTX0007	protein phosphatase 2A, regulatory subunit B, delta isoform	74218800	**0.047**	**–1.3**	**0.047**	**1.37**	38513.4	6.14	19
SCTX0098	protein phosphatase 1, catalytic subunit, beta isoform	74177585	0.91	1.01	**0.049**	**1.9**	37247.2	5.84	16
SCTX0308	protein phosphatase 1, regulatory (inhibitor) subunit 1B	21536256	0.39	–1.21	**0.0065**	**1.83**	21780.6	4.6	17
SCTX0630	guanosine diphosphate (GDP) dissociation inhibitor 2, isoform CRA_b	74150721	0.78	1.02	**0.041**	**–1.23**	57736.9	8.17	25
SCTX0692	mitogen activated protein kinase kinase 2, isoform CRA_e	22122615	0.37	1.15	**0.048**	**–1.57**	45800.9	6.24	9
SCTX0734	mitogen activated protein kinase kinase 1	74226698	**0.047**	**1.3**	**0.049**	**–1.38**	43504.3	6.24	3
Synaptic processes									
SCTX0054	dynamin-1	32172431	0.056	–1.1	**0.03**	**1.14**	97644.9	6.59	20
SCTX0271	N-ethylmaleimide sensitive fusion protein attachment protein alpha	13385392	0.48	1.03	**0.049**	**–1.1**	33189.9	5.3	6
SCTX0362	EH-domain containing 3	10181214	**0.046**	**1.24**	**0.049**	**–1.17**	60869.4	6.04	5
SCTX0635	secernin 1	37359832	**0.017**	**–1.2**	0.15	1.38	49110.4	4.82	10
SCTX1408	synuclein, alpha, isoform CRA_b	148666340	0.68	1.06	**0.049**	**1.32**	15600.6	4.83	10

Names of proteins with altered expression level after Aβ treatment are shown in blue, proteins changed after E2-Aβ treatment are in black, and proteins with altered expression level after both Aβ and E2-Aβ treatments are in red. Av. ratio: ratios of protein expression levels were calculated using DeCyder software package, Biological Variance Analysis module, as the fold change between normalized spot volume of EO-ACSF- and EO-Aβ-treated samples or between EO-Aβ- and E2-Aβ-treated samples. Values below zero: decreased protein level after the specific treatment. Av. = Average; MW = molecular weight; PI = isoelectric point; MW and PI as determined by Uniprot database; % Seq.: protein sequence coverage.

and ChAT signals in the ACSF sites (online suppl. fig. 1A, www.karger.com/doi/10.1159/000321119). Injection of Aβ in EO-treated mice induced the loss of both ChAT and calbindin-positive neurons (online suppl. fig. 1B). E2 pretreatment attenuated both ChAT and calbindin-positive neuron loss from the NBM-SI (loss of calbindin-positive neurons in the NBM-SI of EO-treated mice after Aβ injection: $p = 0.0017$; in the E2-treated animals: $p = 0.0461$; but no significant difference between EO- or E2-treated, Aβ-injected sides: $p = 0.2409$). Interestingly, we

observed some calbindin-positive cholinergic neurons in the E2-Aβ-treated mice, but not in E2-ACSF- or EO-Aβ-treated animals (online suppl. fig. 1C).

Discussion

The present study demonstrates that (1) Aβ solutions of different composition have different toxic potential on NBM cholinergic neurons in vivo; (2) pretreatment with E2 protects cholinergic cells and fibers against Aβ toxicity, and (3) Aβ alone or in combination with E2 pretreatment induces specific changes in the brain proteome of mice.

Spherical Aβ1–42 Oligomers Induce Cholinergic Cell Death, but E2 Pretreatment Is Protective against Aβ Toxicity

There is no agreement in the literature as to which Aβ form is the most toxic. Oligomers and fibrils are well known cytotoxins in vivo [42–45], disrupting cholinergic neurotransmission [46]; however, the monomer was found to be neuroprotective in vitro [47]. In the present study, Aβ solution containing mainly monomers (0 h) had no toxic effect on cholinergic neurons (fig. 1, 2). In contrast, we observed increasing cytotoxicity with increasing ratios of particles with 1–2/2–3 nm height. Spherical Aβ oligomers (observed at 24 and 48 h) induced the maximal neuron loss calculated as the difference between the control and lesioned sites. On the other hand, as the protofibrils were present in the 48-hour solutions but not in the 24-hour ones, we exclude them as the most toxic species on cholinergic neurons. It is important to note that our data do not exclude the possibility that Aβ might affect other neurotransmitter systems. Indeed, injection of Aβ into the NBM induces hypofunction of GABAergic neurons [48] and disturbs the serotonergic innervation of the rat basal forebrain and cerebral cortex [49, 50]. Moreover, as we found loss of calbindin signal in the NBM-SI, but not in cholinergic neurons (online suppl. fig. 1), Aβ indeed regulated also other neurons, such as glutamatergic or GABAergic cells [51, 52].

Although clinical evidence is still controversial, it is well accepted that protection by E2 may vary with dose and timing of the treatment in vivo and in vitro [53]. E2 provides protection even two hours after the insult by rapid activation of signaling pathways and antioxidant mechanisms [54, 55]. Furthermore, E2 pretreatment develops cellular tolerance by inducing gene transcription and protein synthesis [23, 56, 57]. This fine-tuning includes changes in metabolism and synthesis of anti-apoptotic and antioxidant proteins [58]. In the present study, although a single injection of E2 was not enough to increase the basal number of cholinergic neurons or cortical fiber density [59], it was able to reduce the toxic effect of Aβ (fig. 2c, d). However, in contrast to in vitro experiments by others [60], in our study E2 could not eliminate cellular Aβ toxicity or induce further regeneration of cortical projections (fig. 2d). Contrary to our data, in another study [59] a 2-week E2 treatment of rats enhanced cortical cholinergic projections but did not affect the excitotoxicity-induced relative lesion. However, in this study, prolonged E2 treatment more likely increases regeneration than a single injection 24 h before the Aβ exposure. Moreover, injection of N-methyl-D-aspartate (NMDA) in the NBM resulted in approximately 50% loss of cholinergic neurons; while in our study, a more moderate cholinergic cell loss (approximately 25%) was induced using Aβ. In addition, the most likely different toxic mechanisms induced by Aβ and NMDA can also be responsible for the different results.

Putative Mechanisms of Neurotoxicity and Neuroprotection

We hypothesized that Aβ and E2 induce changes in the proteomes that mediate cell death or protect neurons. Comparison of proteomes of (1) EO-ACSF vs. EO-Aβ, and (2) EO-Aβ vs. E2-Aβ provides information about the neurotoxic effect of (1) Aβ and (2) protective mechanisms of E2 against Aβ toxicity. We analyzed protein changes in the NBM-SI (cell bodies, injection), and changes in the SSCTX (projection). Hereafter, the names of proteins with altered expression are in bold print; see tables 1 and 2. Hypothetical pathways suggested to be influenced by Aβ or E2-Aβ treatment are depicted in figure 4.

Aβ induced upregulation of NADH ubiquinone oxidoreductase, and downregulation of ATP synthase (table 1; fig. 4a) in the NBM-SI. Increased NADH oxidation and decreased ATP production utilizing pH gradient might make mitochondria acidic, deplete ATP and trigger apoptotic signaling [61]. Recently, Rhein et al. [62] have found decreased mitochondrial electron transport complex IV activity, a drop in ATP level and upregulation of complex I proteins in Aβ-transgenic mice. These data are in line with the detected changes in our experiment. On the other hand, E2 pretreatment prevented the Aβ-induced regulation of these proteins, preserving mitochondrial integrity. Mitochondrial dysfunction is often associated with increased production of reactive oxygen species inducing inactivation of proteins of the respira-

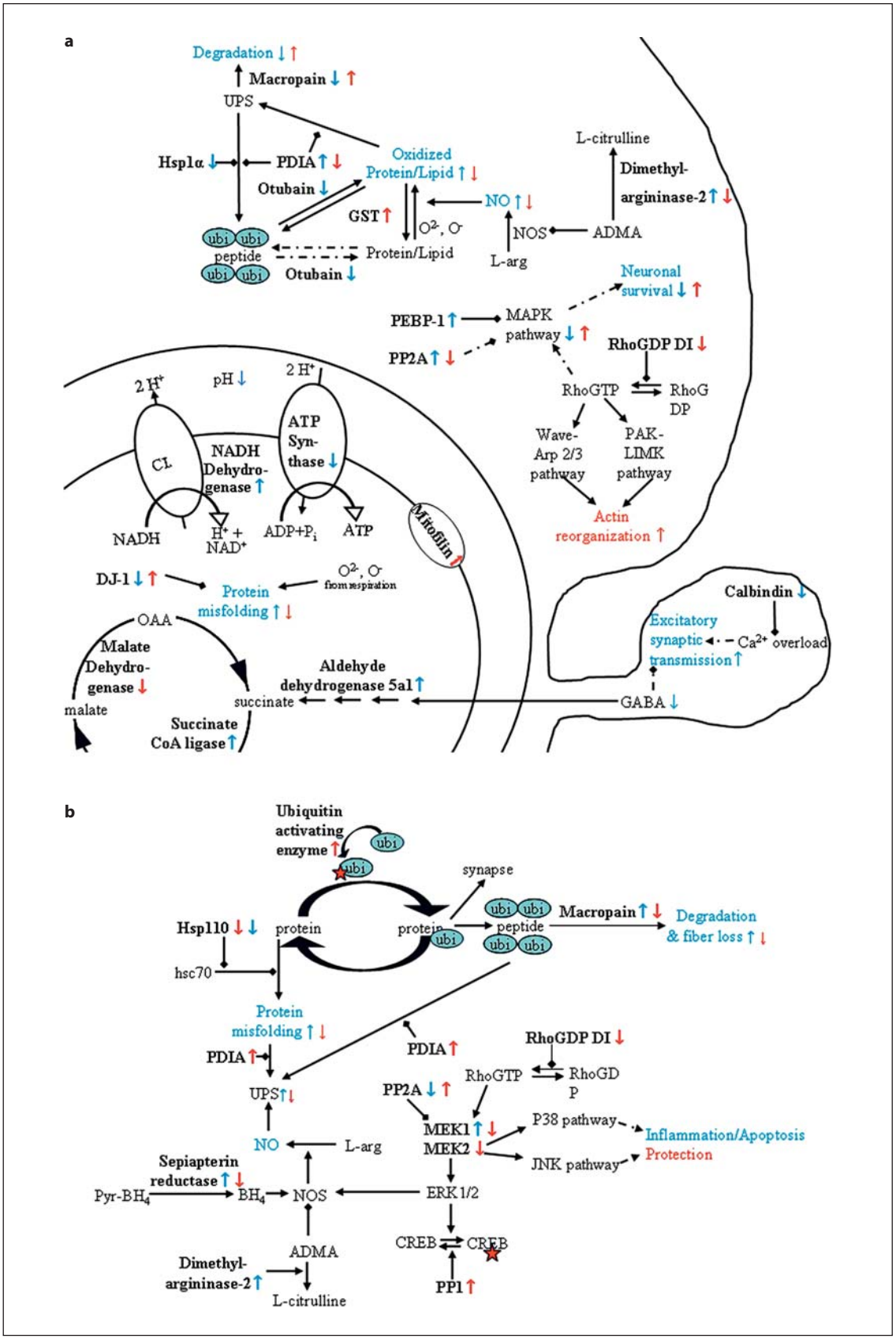
a
Degradation ↓ ↑
Macropain ↓ ↑
UPS
Hsp1α ↓
PDIA ↑ ↓
Otubain ↓
Oxidized Protein/Lipid ↑ ↓
GST ↑
NO ↑ ↓
O2-, O-
ubi ubi peptide ubi ubi
Protein/Lipid
Otubain ↓
NOS
L-arg
ADMA
L-citrulline
Dimethyl-argininase-2 ↑ ↓
Neuronal survival ↓ ↑
PEBP-1 ↑
MAPK pathway ↓ ↑
PP2A ↑ ↓
RhoGDP DI ↓
RhoGTP
RhoGDP
Wave-Arp 2/3 pathway
PAK-LIMK pathway
Actin reorganization ↑
2 H+
pH ↓
2 H+
CL
NADH Dehydro-genase ↑
ATP Syn-thase ↓
NADH
H+ + NAD+
ADP+Pi
ATP
Mitofilin ↑
DJ-1 ↓ ↑
Protein misfolding ↑ ↓
O2-, O- from respiration
OAA
Malate Dehydro-genase ↓
malate
Succinate CoA ligase ↑
succinate
Aldehyde dehydrogenase 5a1 ↑
GABA ↓
Calbindin ↓
Excitatory synaptic transmission ↑
Ca2+ overload
b
Ubiquitin activating enzyme ↑
ubi
synapse
Hsp110 ↓ ↓
protein
hsc70
protein
peptide
Macropain ↑ ↓
Degradation & fiber loss ↑ ↓
Protein misfolding ↑ ↓
PDIA ↑
PDIA ↑
RhoGDP DI ↓
RhoGTP
RhoGDP
UPS ↑ ↓
PP2A ↓ ↑
MEK1 ↑ ↓
MEK2 ↓
P38 pathway
JNK pathway
Inflammation/Apoptosis
Protection
NO
L-arg
Sepiapterin reductase ↑ ↓
Pyr-BH4
BH4
NOS
ERK1/2
ADMA
Dimethyl-argininase-2 ↑
L-citrulline
CREB
CREB
PP1 ↑

tory chain, as it was shown in vivo [62]. Moreover, oxidative inactivation of neuronal proteins may lead to the development of AD [63]. In our experiments, Aβ decreased the level of DJ-1 protein, a chaperon which protects mitochondrial complex I under oxidative stress [64]. Moreover, Aβ increased the expression of dimethylargininase-2, an enzyme that hydrolyses asymmetric dimethylarginine (ADMA) [65]. As ADMA is an endogenous inhibitor of nitrogen monoxide synthase [66], Aβ could trigger NO production and induce further oxidative damage. E2, in turn, increased DJ-1, decreased dimethylargininase-2 and increased glutathione S-transferase expression (fig. 3a). Neurons are particularly susceptible to NO and peroxynitrite exposure, and the nitrosative stress may depend on the level of reduced glutathione [67]. Therefore, E2 pretreatment might reduce nitrosative stress in the NBM.

Signaling pathways associated with raf kinases plays a role in neuronal survival and death signaling. We found upregulation of two raf kinase inhibiting proteins following Aβ treatment, namely phosphatidylethanolamine-binding protein 1 or Raf kinase inhibitor protein (RKIP) and protein phosphatase 2A (PP2A) [68, 69]. The possible inactivation of ERK1/2, p38 or JNK pathways is in contrast to some studies reporting Aβ-induced pathological activation of raf pathways [70, 71]. Contrary to our work, Aβ induced rapid ERK1/2 phosphorylation in vitro [71], or a delayed (48 h) p38MAPK pathway activation in microglia cells in vivo [70], suggesting that ERK pathways mediate rather death than survival signaling following Aβ exposure. The possible differences observed in our studies can be due to the different exposure time, timing of measurements after Aβ application, Aβ concentration, species and the different signals measured (phosphorylation vs. inhibitor expression). Furthermore, we could not detect delayed, increased phosphorylation of p42/44 or p38MAPKs 2 weeks after Aβ injection in the NBM (data not shown). On the other hand, our results and findings from other groups might indicate that Aβ-induced signaling pathway activation can also be time dependent; probably Aβ induced a rapid or delayed activation of these signaling pathways in our study, before or beyond our DIGE experiment (less or more than 24 h). Supporting this latter hypothesis, we found decreased calbindin (CB) expression after Aβ injection. By lowering intracellular Ca^{2+} buffer capacity and increasing Ca^{2+} concentration, decreased calbindin expression could lead to increased MAPK activation in a later time point, and, ultimately, cell death [72, 73]. However, we found no colocalization of CB and ChAT signals in the NBM-SI; therefore, Aβ seems to regulate CB expression in other types of neurons or in glia cells. As significant proportions of the CB-positive cells are likely the cortically projecting, possibly glutamatergic NBM neurons [52], increased intracellular Ca^{2+} concentration due to the loss of CB might induce excitotoxicity in the cortex, and contribute to cholinergic fiber loss and fiber-loss-induced dying back mechanism (fig. 3a). On the other hand, E2 prevented RKIP upregulation and calbindin downregulation and further decreased PP2A expression, decreasing MAPK pathway inhibition. E2 also attenuated calbindin-positive cell loss from the NBM-SI (online suppl. fig. 1). Previously, we demonstrated that rapid action of E2 in vivo involves MAPK signaling in the NBM-SI in vivo [40], and a link has been shown to exist between the neuroprotective effect of E2 and MAPK activation [57]. Altogether, Aβ alters respiration, metabolism and signaling systems of NBM-SI neurons, and these additive effects might all converge on death pathways [74], but can be reduced by E2 pretreatment.

Interestingly, injection of Aβ into the NBM-SI induced protein changes also in the cortical projection area. We found upregulation of sepiapterin reductase, an enzyme essential for tetrahydrobiopterin (cofactor for all NOS isoforms), and dimethylarginine dimethylaminohydrolase 1, a protein that increases NO production (fig. 3b). However, E2 prevented Aβ-dependent upregulation of both enzymes in the SSCTX.

Fig. 4. Schematic illustration of pathways supposed to be regulated by Aβ and/or E2 treatment. **a** We assume that Aβ injection in the NBM-SI increases mitochondrial acidity NADH-dehydrogenase, ATP synthase and decreases DJ-1 expression. Aβ might inhibit MAPK signaling PP2A, PDEBP-1. E2 prevented the regulation of these proteins. **b** Aβ injection in the NMB induced decreased MAPK pathway inhibition PP2A, MEK1 and increased NOS activation sepiapterin reductase, dimethylargininase-2. However, 24 h E2 pretreatment rather led to decreased MAPK signaling PP2A, PP1, RhoGDI MEK1, MEK2 and inhibited NOS activation after Aβ treatment. Names of proteins with altered expression are in bold, and protein regulation by Aβ is indicated with a blue arrow and by E2 with a red arrow. Continuous/dashed arrows indicate direct/indirect regulation, respectively. UPS = Ubiquitin-proteasome system; Hsp = heat shock protein; PDIA = protein disulfide isomerase associated; ubi = ubiquitin; GST = glutathione S-transferase; NOS = nitrogen oxide synthase; ADMA = asymmetric dimethylarginine; PEBP-1 = phosphatidylethanolamine binding protein 1; PP = protein phosphatase; RhoGDP DI = Rho-GDP dissociation inhibitor; MAPK = mitogen-activated protein kinase; BH4 = tetrahydrobiopterin; MEK = MAP kinase kinase 1.

Aβ induced the upregulation of MAP kinase kinase 1 (MEK1) in the SSCTX and in this way – contrary to the findings in the NBM – Aβ may activate ERK1/2, p38 or JNK pathways. Although MEK-activated pathways are often associated with survival and neuroprotection even in in vivo models [75], Aβ also activates the MAPK cascade [76] inducing pathologic phosphorylation of cytoskeletal proteins. We injected the Aβ in the NBM, and we found ERK pathway upregulation just in the projection area, but not in the NBM. These results suggest that Aβ-induced signaling pathway activation is probably regulated with different timing in the two areas. Aβ might induce first a rapid activation in the site of injection (NBM, as suggested in Young et al. [71]), then decrease signaling in the NMB but increase signaling in the projection area, SSCTX (24 h). In addition, inhibition or permanent activation of the same pathway might induce the same response [77, 78]. However, E2 prevented the change in MEK1 expression, and decreased MEK2 level. Moreover, E2 almost doubled the expression of protein phosphatase 1 (PP1) and PP2A, proteins responsible among others for inactivation of some MAPK targets. Similar to our data from the cortex, Valles et al. [20] found that Aβ induced upregulation of the p38MAPK pathway, whereas this activation was prevented by E2 pretreatment. In addition, E2 was shown to induce phosphatases to exert a neuroprotective effect in vitro [79]. Therefore, under these conditions, E2 was able to reverse the proposed Aβ-induced kinase overactivation in the SSCTX (fig. 3b), and probably partly via prevention of cortical fibers and inhibiting 'dying back' process, E2 protected cholinergic cell bodies in the NBM-SI.

It is well known that BFC neurons play an important role in learning and memory formation and that E2 depletion is associated with the cognitive decline observed in AD [24]. In the present study, we demonstrated that E2 is able to reduce Aβ-induced damage in the NBM-SI. We found several cellular processes including regulation of mitochondrial enzymes and signaling pathways that could explain extracellular Aβ toxicity and E2 protection. Collectively, our results demonstrate that in respect to Aβ, multiple factors converge upon pathways of both Aβ-mediated cholinergic neurodegeneration and E2-mediated protection.

Acknowledgments

We are grateful to Péter Batáry for the assistance in statistical analysis. We thank Márta Zarándi (Department of Medical Chemistry, University of Szeged) for generously providing the amyloid-β peptide. This work was supported by the Regional Center of Excellence – Neurobiological Center of Excellence in Southern Hungary (RET-DNK to G.D.J., B.P. and T.J.), by OTKA (68464, 81950 to J.K.), by ETT (to I.M.A.), by the Hungarian National Office of Research and Technology (NANOAMI KFKT-1-2006-0021, OMFB-380/2006 to I.M.K.) and by the Deutsche Forschungsgemeinschaft through the DFG Research Center for Molecular Physiology of the Brain (CMPB, to E.M.S.). We thank András Czurkó and Zsolt Datki for the helpful discussion, and Cathy Ludwig for critical reading of the manuscript.

Author Contributions

E.M.S., G.D.J. and J.K. designed the study. E.M.S. performed the in vivo experiments, tissue staining, DIGE and data analysis. K.A.K. performed DIGE analysis. J.K. performed and analyzed AFM data, Ü.M. and M.S.Z.K. performed ThioflavinT and AFM measurements, B.P. provided the amyloid peptide, and A.C. and T.J. identified the proteins. M.P. prepared the micropunches and G.M. and I.M.A. prepared histochemical staining. E.M.S. and G.D.J. wrote the manuscript.

Disclosure Statement

The authors have no conflicts of interest to disclose.

References

1 Wimo A, Winblad B, Aguero-Torres H, von Strauss E: The magnitude of dementia occurrence in the world. Alzheimer Dis Assoc Disord 2003;17:63–67.

2 Mattson MP: Pathways towards and away from Alzheimer's disease. Nature 2004;430:631–639.

3 Schliebs R, Arendt T: The significance of the cholinergic system in the brain during aging and in Alzheimer's disease. J Neural Transm 2006;113:1625–1644.

4 Mufson EJ, Counts SE, Perez SE, Ginsberg SD: Cholinergic system during the progression of Alzheimer's disease: therapeutic implications. Expert Rev Neurother 2008;8:1703–1718.

5 Wang HY, Lee DHS, Davis CB, Shank RP: Amyloid peptide a beta(1–42) binds selectively and with picomolar affinity to alpha 7 nicotinic acetylcholine receptors. J Neurochem 2000;75:1155–1161.

6 Hernandez CM, Kayed R, Zheng H, Sweatt JD, Dineley KT: Loss of alpha 7 nicotinic receptors enhances beta-amyloid oligomer accumulation, exacerbating early-stage cognitive decline and septohippocampal pathology in a mouse model of Alzheimer's disease. J Neurosci 2010;30:2442–2453.

7 Dineley KT: Beta-amyloid peptide – nicotinic acetylcholine receptor interaction: the two faces of health and disease. Front Biosci 2007;12:5030–5038.

8 Pike CJ, Carroll JC, Rosario ER, Barron AM: Protective actions of sex steroid hormones in Alzheimer's disease. Front Neuroendocrinol 2009;30:239–258.
9 Waring SC, Rocca WA, Petersen RC, O'Brien PC, Tangalos EG, Kokmen E: Postmenopausal estrogen replacement therapy and risk of AD – a population-based study. Neurology 1999;52:965–970.
10 Hu L, Yue Y, Zuo P-p, Jin Z-y, Feng F, You H, li M-L, Ge Q-S: Evaluation of neuroprotective effects of long-term low dose hormone replacement therapy on postmenopausal women brain hippocampus using magnetic resonance scanner. Chin Med Sci J 2006;21: 214–218.
11 Asthana S, Craft S, Baker LD, Raskind MA, Birnbaum RS, Lofgreen CP, Veith RC, Plymate SR: Cognitive and neuroendocrine response to transdermal estrogen in postmenopausal women with Alzheimer's disease: results of a placebo-controlled, double-blind, pilot study. Psychoneuroendocrinology 1999;24:657–677.
12 Henderson VW, Watt L, Buckwalter JG: Cognitive skills associated with estrogen replacement in women with Alzheimer's disease. Psychoneuroendocrinology 1996;21: 421–430.
13 Simpkins JW, Wen Y, Perez E, Yang SH, Wang XF: Role of nonfeminizing estrogens in brain protection from cerebral ischemia – an animal model of Alzheimer's disease neuropathology. Future of hormone therapy: what basic science and clinical studies teach us. Ann NY Acad Sci 2005;1052:233–242.
14 Singh M, Dykens JA, Simpkins JW: Novel mechanisms for estrogen-induced neuroprotection. Exp Biol Med 2006;231:514–521.
15 Simpkins JW, Singh M: More than a decade of estrogen neuroprotection. Alzheimers Dement 2008;4:S131–S136.
16 Abraham IM, Koszegi Z, Tolod-Kemp E, Szego EM: Action of estrogen on survival of basal forebrain cholinergic neurons: promoting amelioration. Psychoneuroendocrinology 2009;34(suppl 1):S104–S112.
17 Morinaga A, Hirohata M, Ono K, Yamada M: Estrogen has anti-amyloidogenic effects on Alzheimer's beta-amyloid fibrils in vitro. Biochem Biophys Res Commun 2007;359: 697–702.
18 Levin-Allerhand JA, Lominska CE, Wang J, Smith JD: 17Alpha-estradiol and 17beta-estradiol treatments are effective in lowering cerebral amyloid-beta levels in abetaPPSWE transgenic mice. J Alzheimers Dis 2002;4: 449–457.
19 Chen SH, Nilsen J, Brinton RD: Dose and temporal pattern of estrogen exposure determines neuroprotective outcome in hippocampal neurons: therapeutic implications. Endocrinology 2006;147:5303–5313.
20 Valles SL, Borras C, Gambini J, Furriol J, Ortega A, Sastre J, Pallardo FV, Vina J: Oestradiol or genistein rescues neurons from amyloid beta-induced cell death by inhibiting activation of p38. Aging Cell 2008;7:112–118.
21 Rasgon NL, Silverman D, Siddarth P, Miller K, Ercoli LM, Elman S, Lavretsky H, Huang SC, Phelps ME, Small GW: Estrogen use and brain metabolic change in postmenopausal women. Neurobiol Aging 2005;26:229–235.
22 Brinton RD: Estrogen regulation of glucose metabolism and mitochondrial function: Therapeutic implications for prevention of Alzheimer's disease. Adv Drug Deliv Rev 2008;60:1504–1511.
23 Szego EM, Kekesi KA, Szabo Z, Janaky T, Juhasz GD: Estrogen regulates cytoskeletal flexibility, cellular metabolism and synaptic proteins: a proteomic study. Psychoneuroendocrinology 2010;35:807–819.
24 Gibbs RB: Does short-term estrogen therapy produce lasting benefits in brain? Endocrinology 2010;151:843–845.
25 Leuner B, Mendolia-Loffredo S, Shors TJ: High levels of estrogen enhance associative memory formation of ovariectomized females. Psychoneuroendocrinology 2004;29: 883–890.
26 Henderson VW, Paganini-Hill A, Miller BL, Elble RJ, Reyes PF, Shoupe D, McCleary CA, Klein RA, Hake AM, Farlow MR: Estrogen for Alzheimer's disease in women – randomized, double-blind, placebo-controlled trial. Neurology 2000;54:295–301.
27 Wang PN, Liao SQ, Liu RS, Liu CY, Chao HT, Lu SR, Yu HY, Wang SJ, Liu HC: Effects of estrogen on cognition, mood, and cerebral blood flow in AD – a controlled study. Neurology 2000;54:2061–2066.
28 Manthey D, Behl C: From structural biochemistry to expression profiling: neuroprotective activities of estrogen. Neuroscience 2006;138:845–850.
29 Joerchel S, Raap M, Bigl M, Eschrich K, Schliebs R: Oligomeric beta-amyloid(1–42) induces the expression of Alzheimer disease-relevant proteins in cholinergic sn56.B5.G4 cells as revealed by proteomic analysis. Int J Dev Neurosci 2008;26:301–308.
30 Prokai L, Stevens SM, Rauniyar N, Nguyen V: Rapid label-free identification of estrogen-induced differential protein expression in vivo from mouse brain and uterine tissue. J Proteome Res 2009;8:3862–3871.
31 Aluise CD, Robinson RA, Beckett TL, Murphy MP, Cai J, Pierce WM, Markesbery WR, Butterfield DA: Preclinical Alzheimer disease: brain oxidative stress, Abeta peptide and proteomics. Neurobiol Dis 2010;39:221–228.
32 Zarandi M, Soos K, Fulop L, Bozso Z, Datki Z, Toth GK, Penke B: Synthesis of a beta(1–42) and its derivatives with improved efficiency. J Pept Sci 2007;13:94–99.
33 Stine WB, Dahlgren KN, Krafft GA, LaDu MJ: In vitro characterization of conditions for amyloid-beta peptide oligomerization and fibrillogenesis. J Biol Chem 2003;278: 11612–11622.
34 Harper JD, Wong SS, Lieber CM, Lansbury PT: Observation of metastable A beta amyloid protofibrils by atomic force microscopy. Chem Biol 1997;4:119–125.
35 Naiki H, Gejyo F: Kinetic analysis of amyloid fibril formation: amyloid, prions, and other protein aggregates. Methods Enzymol 1999; 309:305–318.
36 Paxinos G, Franklin KBJ: The Mouse Brain in Stereotaxic Coordinates. San Diego, Academic Press, 2001.
37 Palkovits M: Isolated removal of hypothalamic or other brain nuclei of rat. Brain Res 1973;59:449–450.
38 Palkovits M, Brownstein MJ: Maps and Guide to Microdissection of the Rat Brain. New York, Elsevier, 1988.
39 Kapp EA, Schutz F, Reid GE, Eddes JS, Moritz RL, O'Hair RAJ, Speed TP, Simpson RJ: Mining a tandem mass spectrometry database to determine the trends and global factors influencing peptide fragmentation. Anal Chem 2003;75:6251–6264.
40 Szego EM, Barabas K, Balog J, Szilagyi N, Korach KS, Juhasz G, Abraham IM: Estrogen induces estrogen receptor alpha-dependent camp response element-binding protein phosphorylation via mitogen-activated protein kinase pathway in basal forebrain cholinergic neurons in vivo. J Neurosci 2006;26: 4104–4110.
41 Hedreen JC, Bacon SJ, Price DL: A modified histochemical technique to visualize acetylcholinesterase-containing axons. J Histochem Cytochem 1985;33:134–140.
42 Cleary JP, Walsh DM, Hofmeister JJ, Shankar GM, Kuskowski MA, Selkoe DJ, Ashe KH: Natural oligomers of the amyloid-protein specifically disrupt cognitive function. Nat Neurosci 2005;8:79–84.
43 Shankar GM, Li SM, Mehta TH, Garcia-Munoz A, Shepardson NE, Smith I, Brett FM, Farrell MA, Rowan MJ, Lemere CA, Regan CM, Walsh DM, Sabatini BL, Selkoe DJ: Amyloid-beta protein dimers isolated directly from Alzheimer's brains impair synaptic plasticity and memory. Nat Med 2008;14: 837–842.
44 Lesne S, Koh MT, Kotilinek L, Kayed R, Glabe CG, Yang A, Gallagher M, Ashe KH: A specific amyloid-beta protein assembly in the brain impairs memory. Nature 2006;440: 352–357.
45 Busciglio J, Lorenzo A, Yeh J, Yankner BA: Beta-amylid fibrils induce tau-phosphorylation and loss of microtubule-binding. Neuron 1995;14:879–888.

46 Machova E, Rudajev V, Smyckova H, Koivisto H, Tanila H, Dolezal V: Functional cholinergic damage develops with amyloid accumulation in young adult appswe/ps1de9 transgenic mice. Neurobiol Dis 2010;38:27–35.
47 Giuffrida ML, Caraci F, Pignataro B, Cataldo S, De Bona P, Bruno V, Molinaro G, Pappalardo G, Messina A, Palmigiano A, Garozzo D, Nicoletti F, Rizzarelli E, Copani A: Beta-amyloid monomers are neuroprotective. J Neurosci 2009;29:10582–10587.
48 Scali C, Prosperi C, Giovannelli L, Bianchi L, Pepeu G, Casamenti F: Beta(1–40) amyloid peptide injection into the nucleus basalis of rats induces microglia reaction and enhances cortical gamma-aminobutyric acid release in vivo. Brain Res 1999;831:319–321.
49 Harkany T, O'Mahony S, Keijser J, Kelly JP, Konya C, Borostyankoi ZA, Gorcs TJ, Zarandi M, Penke B, Leonard BE, Luiten PGM: Beta-amyloid((1–42))-induced cholinergic lesions in rat nucleus basalis bidirectionally modulate serotonergic innervation of the basal forebrain and cerebral cortex. Neurobiol Dis 2001;8:667–678.
50 Aguado-Llera D, Arilla-Ferreiro E, Chowen JA, Argente J, Puebla-Jimenez L, Frago LM, Barrios V: 17-Beta-estradiol protects depletion of rat temporal cortex somatostatinergic system by beta-amyloid. Neurobiol Aging 2007;28:1396–1409.
51 Gonzalez I, Arevalo-Serrano J, Perez JL, Gonzalo P, Gonzalo-Ruiz A: Effects of beta-amyloid peptide on the density of m2 muscarinic acetylcholine receptor protein in the hippocampus of the rat: relationship with gaba-, calcium-binding protein and somatostatin-containing cells. Neuropathol Appl Neurobiol 2008;34:506–522.
52 Gritti I, Manns ID, Mainville L, Jones BE: Parvalbumin, calbindin, or calretinin in cortically projecting and gabaergic, cholinergic, or glutamatergic basal forebrain neurons of the rat. J Comp Neurol 2003;458:11–31.
53 Gibbs RB: Effects of estrogen on basal forebrain cholinergic neurons vary as a function of dose and duration of treatment. Brain Res 1997;757:10–16.
54 Shughrue PJ, Merchenthaler I: Estrogen prevents the loss of ca1 hippocampal neurons in gerbils after ischemic injury. Neuroscience 2003;116:851–861.
55 Merchenthaler I, Shughrue PJ: Neuroprotection by estrogen in animal models of ischemia and Parkinson's disease. Drug Dev Res 2005;66:172–181.
56 Nilsen J, Chen SH, Irwin RW, Iwamoto S, Brinton RD: Estrogen protects neuronal cells from amyloid beta-induced apoptosis via regulation of mitochondrial proteins and function. BMC Neurosci 2006;7:74.
57 Lebesgue D, Chevaleyre V, Zukin RS, Etgen AM: Estradiol rescues neurons from global ischemia-induced cell death: multiple cellular pathways of neuroprotection. Steroids 2009;74:555–561.
58 Garcia-Segura LM, Azcoitia I, DonCarlos LL: Neuroprotection by estradiol. Prog Neurobiol 2001;63:29–60.
59 Horvath KM, Hartig W, Van der Veen R, Keijser JN, Mulder J, Ziegert M, Van der Zee EA, Harkany T, Luiten PGM: 17-Beta-estradiol enhances cortical cholinergic innervation and preserves synaptic density following excitotoxic lesions to the rat nucleus basalis magnocellularis. Neuroscience 2002;110:489–504.
60 Guerra B, Diaz M, Alonso R, Marin R: Plasma membrane oestrogen receptor mediates neuroprotection against beta-amyloid toxicity through activation of raf-1/mek/erk cascade in septal-derived cholinergic sn56 cells. J Neurochem 2004;91:99–109.
61 Yang L, Mei Y, Xie Q, Han X, Zhang F, Gu L, Zhang Y, Chen Y, Li G, Gao Z: Acidification induces bax translocation to the mitochondria and promotes ultraviolet light-induced apoptosis. Cell Mol Biol Lett 2008;13:119–129.
62 Rhein V, Song XM, Wiesner A, Ittner LM, Baysang G, Meier F, Ozmen L, Bluethmann H, Drose S, Brandt U, Savaskan E, Czech C, Gotz J, Eckert A: Amyloid-beta and tau synergistically impair the oxidative phosphorylation system in triple transgenic Alzheimer's disease mice. Proc Natl Acad Sci USA 2009;106:20057–20062.
63 Butterfield DA, Poon HF, St Clair D, Keller JN, Pierce WM, Klein JB, Markesbery WR: Redox proteomics identification of oxidatively modified hippocampal proteins in mild cognitive impairment: Insights into the development of Alzheimer's disease. Neurobiol Dis 2006;22:223–232.
64 Hayashi T, Ishimori C, Takahashi-Niki K, Taira T, Kim YC, Maita H, Maita C, Ariga H, Iguchi-Ariga SMM: Dj-1 binds to mitochondrial complex i and maintains its activity. Biochem Biophys Res Commun 2009;390:667–672.
65 Smith MA, Harris PLR, Sayre LM, Beckman JS, Perry G: Widespread peroxynitrite-mediated damage in Alzheimer's disease. J Neurosci 1997;17:2653–2657.
66 Leiper J, Vallance P: Biological significance of endogenous methylarginines that inhibit nitric oxide synthases. Cardiovasc Res 1999;43:542–548.
67 Calabrese V, Boyd-Kimball D, Scapagnini G, Butterfield DA: Nitric oxide and cellular stress response in brain aging and neurodegenerative disorders: the role of vitagenes. In Vivo 2004;18:245–267.
68 Granovsky AE, Rosner MR: Raf kinase inhibitory protein: a signal transduction modulator and metastasis suppressor. Cell Res 2008;18:452–457.
69 Zhao J, Wu HW, Chen YJ, Tian HP, Li LX, Han X, Guo J: Protein phosphatase 2a-negative regulation of the protective signaling pathway of Ca^{2+}/cam-dependent erk activation in cerebral ischemia. J Neurosci Res 2008;86:2733–2745.
70 Giovannini MG, Scali C, Prosperi C, Bellucci A, Vannucchi MG, Rosi S, Pepeu G, Casamenti F: Beta-amyloid-induced inflammation and cholinergic hypofunction in the rat brain in vivo: involvement of the p38mapk pathway. Neurobiol Dis 2002;11:257–274.
71 Young KF, Pasternak SH, Rylett RJ: Oligomeric aggregates of amyloid beta peptide 1–42 activate erk/mapk in sh-sy5y cells via the alpha 7 nicotinic receptor. Neurochem Int 2009;55:796–801.
72 Christakos S, Liu Y: Biological actions and mechanism of action of calbindin in the process of apoptosis. J Steroid Biochem Mol Biol 2004;89–90:401–404.
73 Geula C, Bu J, Nagykery N, Scinto LFM, Chan J, Joseph J, Parker R, Wu CK: Loss of calbindin-d-28k from aging human cholinergic basal forebrain: relation to neuronal loss. J Comp Neurol 2003;455:249–259.
74 Ferrer I: Altered mitochondria, energy metabolism, voltage-dependent anion channel, and lipid rafts converge to exhaust neurons in Alzheimer's disease. J Bioenerg Biomembr 2009;41:425–431.
75 Sawe N, Steinberg G, Zhao H: Dual roles of the mapk/erk1/2 cell signaling pathway after stroke. J Neurosci Res 2008;86:1659–1669.
76 Matos M, Augusto E, Oliveira CR, Agostinho P: Amyloid-beta peptide decreases glutamate uptake in cultured astrocytes: involvement of oxidative stress and mitogen-activated protein kinase cascades. Neuroscience 2008;156:898–910.
77 Calabrese EJ, Baldwin LA: Hormesis: U-shaped dose responses and their centrality in toxicology. Trends Pharmacol Sci 2001;22:285–291.
78 Marini AM, Jiang H, Pan H, Wu X, Lipsky RH: Hormesis: A promising strategy to sustain endogenous neuronal survival pathways against neurodegenerative disorders. Ageing Res Rev 2008;7:21–33.
79 Simpkins JW, Yi KD, Yang SH: Role of protein phosphatases and mitochondria in the neuroprotective effects of estrogens. Front Neuroendocrinol 2009;30:93–105.